Cobalt immobilization performance and mechanism analysis of low carbon belite calcium sulfoaluminate cement

Chi, Lin; Li, Mengxuan; Zhang, Qianrui; Liang, Xuhui; Huang, Chendong; Peng, Bin; Sun, Haisheng

DOI
10.1016/j.conbuildmat.2023.131545

Publication date
2023

Document Version
Final published version

Published in
Construction and Building Materials

Citation (APA)
Chi, L., Li, M., Zhang, Q., Liang, X., Huang, C., Peng, B., & Sun, H. (2023). Cobalt immobilization performance and mechanism analysis of low carbon belite calcium sulfoaluminate cement. *Construction and Building Materials*, *386*, Article 131545. https://doi.org/10.1016/j.conbuildmat.2023.131545

Construction and Building Materials 386 (2023) 131545

Contents lists available at ScienceDirect

Construction and Building Materials

journal homepage: www.elsevier.com/locate/conbuildmat

Cobalt immobilization performance and mechanism analysis of low carbon belite calcium sulfoaluminate cement

Lin Chi [a], Mengxuan Li [a], Qianrui Zhang [a], Xuhui Liang [b,*], Chendong Huang [a], Bin Peng [a,*], Haisheng Sun [a]

[a] School of Environment and Architecture, University of Shanghai for Science and Technology, Shanghai 200093, China
[b] Department of Materials, Mechanics, Management & Design, Faculty of Civil Engineering and Geoscience, Delft University of Technology, Delft, the Netherlands

ARTICLE INFO

Keywords:
Belite calcium sulfoaluminate cement
Cobalt immobilization
Cement hydration
Hazardous waste

ABSTRACT

Cementitious materials are well acknowledged as one of the most adaptable materials for immobilizing heavy metals. Belite calcium sulfoaluminate cement (BCSA), one of the low-carbon alternative binders to cement with superior properties regarding chemical resistance and mechanical properties, is found with a desirable capability for waste immobilization. In this study, BCSA was used for Co(II) immobilization with a dosage of up to 2.5% by weight of BCSA. The results showed that Co(II) could promote the hydration of BCSA pastes, specifically accelerated the hydration of ye'elimite. More hydration products could be generated in the Co(II)-doped BCSA pastes, leading to the construction of a denser microstructure. The compressive strength of BCSA pastes would be slightly improved when BCSA was used for Co(II) immobilization, and the electrical resistivity would decrease. In terms of Co(II) immobilization, BCSA cement exhibited a desirable capacity for Co(II) immobilization. The majority of the Co(II) could be immobilized within the first 100 min of mixing BCSA with Co(II) solutions. The immobilization degrees of Co(II) in hardened BCSA pastes could approach about 99.99% after 7d. The acquired results indicated that BCSA cement is effective for Co(II) immobilization. Therefore, BCSA has a low-carbon advantage with superior strength development over time and prospective capacity of heavy metals immobilization.

1. Introduction

Cobalt is an indispensable metal extensively used in industrial manufacturing, such as the production of alloys, catalysts, and lithium-ion batteries. As the demands for those products increases, cobalt-containing products become more accessible. However, the recovery of cobalt during the production as well as after the life span of the cobalt-containing products is less noticed. The excessive accumulation of cobalt into the environment is detrimental to the environment, leading to the contamination of water and land [1]. Due to its chemical toxicity, cobalt poses a significant risk to human health, including diminished lung function, vision problems, thyroid damage, and heart problems in humans [2–4]. Therefore, it is essential for the immobilization of cobalt for the purpose of environmental management.

In addition to limiting the production of cobalt-containing materials, adsorption and/or solidification of the cobalt ions are the primary strategies for reducing the cobalt availability in wastewater [5,6]. Conventionally, the most prevalent techniques are chemical precipitation, reverse osmosis, and ion exchange [7,8]. The lab-synthesized materials such as layered double hydroxides (LDHs) [9,10] and highly dispersed silica gels [11] were discovered to be effective at adsorbing Co (II) from wastewater. However, given its high cost, it is impractical to use pure chemicals for cobalt immobilization from the engineering point of view. In recent decades, research has been conducted on inexpensively cobalt adsorbing agents, e.g., zeolite, clay, and adsorbents prepared with rice husk ash in order to develop additional cobalt removal strategies with a lower cost [12–16].

Cementitious materials are one of the most used man-made materials in the world, with the benefits of low cost and good durability. What mostly striking is that cementitious materials are reported advantageous for heavy metals immobilization. In the Portland cement (OPC) system, Co(II) immobilization degrees can reach 99.7% at 28 days when 70% of the cement is replaced with slag [17]. Cobalt exists in cement matrix in two forms, Co(II) and Co(III). Co(II) would predominantly form Co(II)-

* Corresponding authors.
E-mail addresses: X.Liang-1@tudelft.nl (X. Liang), BinPeng@usst.edu.cn (B. Peng).

https://doi.org/10.1016/j.conbuildmat.2023.131545
Received 20 January 2023; Received in revised form 2 April 2023; Accepted 24 April 2023
Available online 4 May 2023

like hydroxide phases $Co(OH)_2$, Co-LDH, or Co-phyllosilicates, and Co (III) would predominantly form Co(III)O(OH)-like phases or Co-phyllomanganate [18]. Even though a good immobilization degree could be achieved, it was discovered that cobalt would decelerate the hydration of OPC. The immobilization of cobalt could reduce the mechanical strength and further impair the long-term durability of cement, which could lead to a lower immobilization capacity over time [19,20].

In spite of the satisfactory immobilization capacity of OPC with its low cost, the high environmental cost of OPC raises concerns about its widespread use for heavy metal immobilization. The alternative binders with less environmental impact and desirable immobilization capacity are demanding, and calcium sulfoaluminate (CSA) cement is one of the promising candidates. The overall carbon footprint of CSA can be 35% lower than that of OPC [21]. Meanwhile, CSA shows technical advantages such as fast setting, high early strength, desirable chemical resistance, which are desirable for heavy metals immobilization from engineering perspectives as they shorten the working time, achieve good immobilization capacity at early stage, and provide resistance to degradation from the external environment. Ye'elimite is the primary phase in CSA cement and will form ettringite(AFt), monosulfate (AFm), and AH_3 gels once hydration. These reaction products are capable of adsorbing heavy metals. Thus, CSA cement has been widely investigated to immobilize heavy metals. Cr(II), Mn(II),Cd(II), Pb(II) were found to be well encapsulated in CSA cement [22]. Heavy metals could be integrated into the microstructure of hydrates such as AFm or C_4AH_{13} [23]. Belite calcium sulfoaluminate cement (BCSA) is one of the subsidies of CSA cement that primarily contains ye'elimite and belite as the major phases. Compared to conventional CSA cement, BCSA contains a higher proportion of C_2S. The lower requirement of alumina-rich materials in BCSA brings benefits from an economic point of view. Besides, introducing C_2S could promote the formation of C-S-H gels and contribute to the long-term strength development of BCSA. C-S-H gels are also reported with a desirable adsorption capacity for heavy metals [24,25]. Therefore, BCSA has an economic advantage over conventional CSA with superior strength development over time and prospective capacity of heavy metals immobilization.

Despite the fact that considerable research has been conducted to immobilize heavy metals with BCSA [26–28], the implication of BCSA in Co(II) immobilization, to the authors' understanding, is rare. In this work, the immobilization of cobalt with BCSA was investigated. With the characterization techniques including X-ray diffraction (XRD), EIS, and SEM analysis, the mechanisms of cobalt immobilization were elaborated from the microstructure point, aiming to provide a theoretical understanding of Co(II) immobilization in BCSA.

2. Experiment

2.1. Materials

The BCSA cement was supplied by the Polar Bear Building Materials Co., Ltd, Tangshan. The chemical compositions and mineralogical compositions are listed in Table 1. The reference sample (BCSA0) comprised 90% BCSA cement and 10% anhydrite. $Co(NO_3)_2{\bullet}6H_2O$ (AR > 99.7%) supplied by Merck (Germany) was used as the cobalt resource. Deionized water was used for sample preparation. The mixtrue proportions can be found in Table 2. Four gradients (0, 0.5, 1, and 2.5% of BCSA by weight) were applied regarding the concentration of Co(II). To prepare samples, $Co(NO_3)_2{\bullet}6H_2O$ was firstly dissolved in water, then blended with cement to prepare pastes. The reference sample was named BCSA0, and the other groups were named in accordance with their Co(II) concentrations. The water to cement ratio was kept at 0.5 constantly.

Table 1
Chemical and mineralogical composition (wt.%) of BCSA cement.

Chemical composition		Phase composition	
SiO_2	14.16	C_2S	47.25
CaO	49.6	Ye'elimite	41.6
Fe_2O_3	2.69	C_4AF	5.75
Al_2O_3	21.65	$CaSO_4{\cdot}2H_2O$	5.4
Na_2O	0.13		
K_2O	0.25		
MgO	0.96		
SO_3	9.54		
LOI	1.02		

2.2. Experimental methods

2.2.1. Isothermal calorimetry

The heat evolution of BCSA pastes with different amounts of Co(II) was determined by a TAM Air calorimeter (TA Instruments Inc.). The cement powders were filled into the vials and placed into the calorimetric chamber for equilibrium until 12 hours. Then the mixing solutions were injected into the vials for inner-mixing for 5min, and the heat flow of pastes was recorded accordingly. A fixed amount of distilled water with the same specific heat as the pastes were used as the reference group during the test. The environment temperature was 21±1℃ and the heat evolution was recorded up to 72 hrs.

2.2.2. Compressive strength test

Cubic samples with the size of 2×2×2 cm^3 were used for the compressive strength test. Once cast, the fresh pastes were sealed with plastic films to avoid water evaporation. The samples were demolded after 24 hrs, then immersed in the lime-saturated solution, and cured until the strength test. The strength test followed the ASTM C109 standard [29] with a loading rate of 2400±200N/s. Six replicates were tested for each sample.

2.2.3. Microstructure characterization

(1) XRD

The reaction products of pastes were characterized by X-ray diffraction (XRD, Bruker D8 Advance). Cr Kα radiation was applied in this study, and the diffraction degree of 2 thetas spanned from 5° to 65° with a speed rate of 0.02 °/s.

(2) EIS

The resistivity of BCSA cement paste blended with cobalt ions was measured with three electrodes system (working, reference and counter electrode) by the electrochemical workstation (VersaSTAT 4000A, Princeton, USA). The dimensions of the samples are 60 mm × 44 mm× 28 mm. The frequency ranged from 10 MHz to 1 Hz, and the amplitude was set as 100 mV. For each binder, two samples were tested. The resistance of bulk cement paste is obtained according to the equivalent circuit $R[QR][QR]$. The resistivity of cement paste was further calculated by $\rho{=}R$ L/S.

(3) MIP

The pore structure analysis was conducted by using the AutoPore IV 9500 mercury intrusion porosimetry (Micrometritics) with a pressure

Table 2
Mixture proportions of the BCSA cement paste.

Mixtures*	Water/cement ratio	$Co(NO_3)_2{\cdot}6H_2O$ (%)
BCSA0 (Control)	0.5	0
BCSA0.5		0.5
BCSA1		1
BCSA2.5		2.5

ranging from 0 to 32000 psia. The contact angel was set at 130 degrees with the Hg surface tension at 485 dynes/cm.

(4) SEM

A Hitachi S-4800 scanning electron microscope (SEM) was applied to characterize the microstructure of pastes. Due to the poor surface conductivity, the samples were sputtered with carbon coating before the SEM test. The test was conducted at 10 kV accelerating voltage in a high vacuum environment.

2.2.4. Co(II) Leaching and immobilization test

(1) Co(II) immobilization by BCSA cement

0.25 grams of BCSA cement powders were placed in the 100 ml centrifugal bottles and blended with 50 ml of $Co(NO_3)_2$ solutions with a molarity of 16 mM. The centrifugal bottle was placed in the horizontal shaking water bath with a shaking frequency of 200 rpm. 3 mL of supernatants were collected after 100, 200, 400, and 2000 min. The ion concentration of supernatants was determined by Inductively coupled plasma mass spectrometry (ICP-MS, Thermo Fisher Scientific Inc.USA). Two replicates were tested for each ion concentration.

(2) Leachability of Co(II) from BCSA cement pastes at different curing age

The leachability of Co(II) from BCSA pastes was determined using a modified Toxicity Characteristic Leaching Procedure (TCLP). The paste samples were cast into 5 mL centrifuge tubes and vacuum-sealed to prevent carbonation until a predetermined curing age (1 d, 3 d, 7 d, 28 d, 56 d, 90 d). The samples were then demolded, crushed, and ground into powders to pass through the sieves with a diameter of 30 μm. For the leaching test, 2.5 grams of powders were collected and mixed with 50 ml of distilled water. The samples were placed on the horizontal shaking water bath with a shaking frequency of 150 rpm and a constant temperature of 21 ± 1 °C for 24 hrs. Later 5 ml of supernatants were filtered and subjected to determine the concentration of Co(II) through the ICP-MS. The Co(II) ions immobilization degree R could be calculated according to Eq. (1):

$$R = \frac{Co - Ce}{Co} \times 100\% \quad (1)$$

Where C_o (mg/L) and C_e (mg/L) are the initial and final Co(II) concentrations, respectively.

(3) Leachability of Co(II) from BCSA cement paste in different pH

A modified TCLP test was used to determine the leachability of Co(II) and other ions from hardened BCSA pastes at various pH values. BCSA2.5 with a hydration age of 7 d was crushed into powders and passed through a 40 mesh sieve for the test. 2.5 g of the powder samples were dissolved in 50 mL of ionized water. The pH of the solutions ranged from 4.0 to 11.0 and was tailored by the dropwise addition of HCl or NaOH solutions with a molarity of 0.01M. Samples were placed on the horizontal shaking water bath for 72 hrs, and the ions concentration was obtained through ICP-MS.

3. Results and discussion

3.1. Isothermal calorimetry

The isothermal exothermic curves of BSCA pastes with different amounts of Co(II) are shown in Fig. 1. Consistent with previous research, the hydration of BSCA could be in general distinguished with four stages

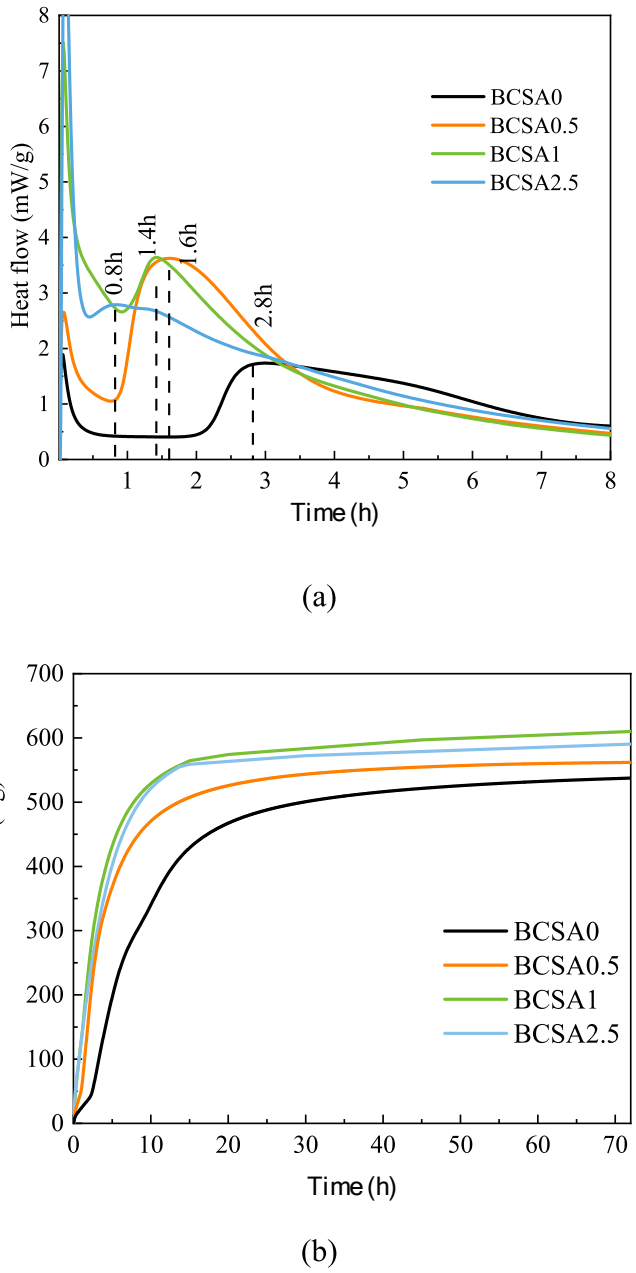

Fig. 1. Heat flow (a) and cumulative heat (b) of BCSA pastes with various amounts of Co(II).

based on the heat flow curve [30]. BSCA pastes containing Co(II) were found with similar hydration processes in terms of the four-stage feature, but each step exhibited distinct characteristics.

The first stage, referred to as the dissolution period, was characterized by an exothermal peak with high intensity within the first few minutes, and is assumed to be related to the wetting and dissolution of cement particles [31,32]. It can be clearly seen that pastes with a higher amount of Co(II) had a larger absolute value for heat flow, indicating that the dissolution of BCSA cement was accelerated with the incorporation of Co(II). The initial dissolution of BCSA led to an increase in ion concentrations, which led to the formation of reaction products on the surface of anhydrous particles that impeded the dissolution of cement particles [31]. As a result, the hydration reached the second stage, i.e., the induction period. The reaction proceeded mildly and slowly at this stage as the dissolution rate slowed. The duration of the induction period of the reference sample (BCSA 0) was approximately 1.5 hrs. Notably,

the induction period of pastes became shorter with the increment of Co (II) concentration, and no clear induction period could be observed for BCSA 2.5. This could be explained, on the one hand, by the fact that the acidity of $Co(NO_3)_2$ in nature would neutralize the alkalinity of pore solutions, resulting in the continued dissolution of clinker phases. In addition, as Co(II) accelerated the dissolution of BCSA in the first stage, a large amount of initial reaction products could play a role as the nucleation site to promote the precipitation of hydration products, leading to the presence of the second exothermic peak [33].

The third stage was the acceleration period, which could be identified by the increasing heat flow with a second exothermic peak. The high heat flow resulted from the precipitation of a large amount of hydration products (ettringite and AH_3 gels), and the main hydration reaction followed Eq. (2). With the addition of Co(II), the time required for each mixture to reach the second exothermic peak, as indicated in Fig. 1(a), was shorter. Specifically, it took about 2.8, 1.6. 1.4, and 0.8 hrs to reach the second exothermic peak for pastes BCSA0, BCSA0.5, BCSA1, and BCSA2.5. This result confirmed that Co(II) promoted the hydration process of BCSA cement with more hydration products generated. The last stage referred to the deceleration period, where the reaction mainly involved with the continuous dissolution of cement and precipitation of hydration products.

$$C_4A_3\overline{S} + 2C\overline{S} + 38H \rightarrow C_3A{\cdot}3C\overline{S}{\cdot}H_{32} + 2AH_3 \quad (2)$$

The cumulative heat of pastes shown in Fig. 1(b) revealed that Co(II) would lead to a large exothermic heat during the hydration of BCSA. Since the cumulative heat was proportional to the hydration degree of cement [34], it could be expected, therefore, that Co(II)-doped BCSA cement paste could achieve a higher hydration degree than the reference sample, and a higher amount of reaction products can be generated in pastes with Co(II).

3.2. Microstructure analysis

3.2.1. XRD analysis

The XRD patterns of BCSA0 and BCSA2.5 at 3d, 7d, and 28d are shown in Fig. 2, and the main crystalline phases are marked accordingly. As can be seen, besides the clinker phases, i.e., anhydrite, ye'elimite, and C_2S, the main hydration products in the BCSA pastes were ettringite (AFt) in all the BCSA pastes. The excess of anhydrite in the mixture design assured that ettringite was the principal hydration products and that no monosulfate would be generated. The diffraction peak of ettringite remaining unchanged before and after Co(II) immobilization suggests that the minor integration of Co(II) into ettringite did not significantly impact its lattice structure. This has also been reported elsewhere with other heavy metals [35–37]. A minor diffraction peak at the 2 thetas of 11.7° was discovered, which could be attributed to the presence of Ca-Al LDH (monocarboaluminate) [38,39]. The other main hydration products, AH_3 gels that were widely reported in the literature [40,41], however, can hardly be identified in the XRD pattern due to its amorphous structure. As for the hydration products for belite, however, it is difficult to observe the diffraction peaks for either portlandite nor C-S-H gels. This is due to the slow reaction of belite in a low alkalinity environment, which results in limited precipitation of reaction products. Additionally, C-S-H gels cannot be detected by XRD because of their poor crystallinity. These results are consistent with previous research

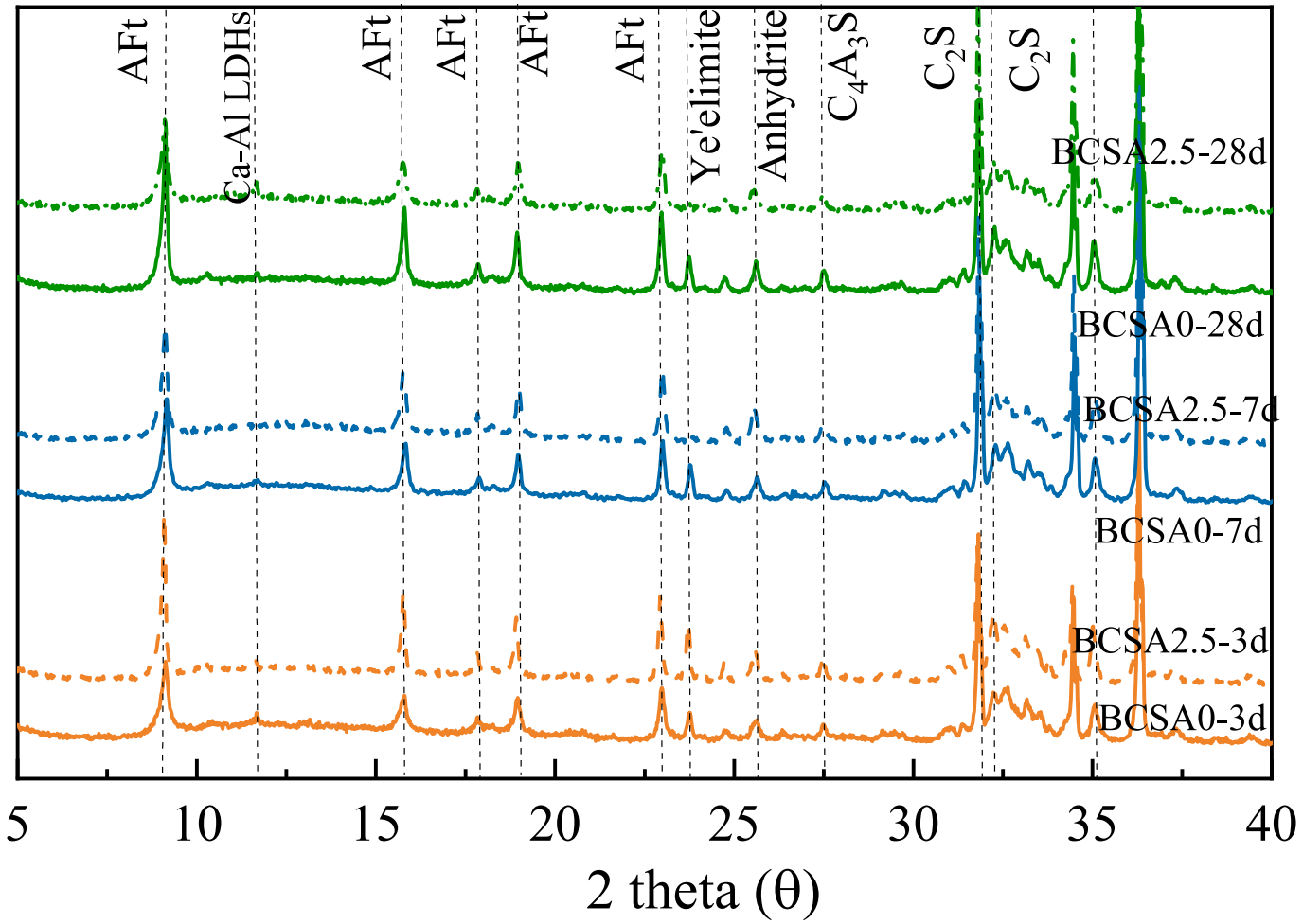

Fig. 2. XRD patterns of BCSA 0 and BCSA 2.5 at 3d, 7d, and 28d.

[42,43].

By comparing the XRD pattern of BCSA 0 and BCSA 2.5, it was interesting to observe that starting from 7d, the diffraction peak of ye'elimite was not visible in BCSA 2.5 but still can be seen in BCSA 0 even at 28d. It could be deduced, therefore, that Co(II) promoted the hydration of BCSA, especially ye'elimite, and leading to a higher amount of reaction products generation including ettringite and possibly AH_3 gels according to Eq. (2). This result was also in agreement with the isothermal calorimetry test that Co(II)-doped BCSA was expected to have a higher reaction degree.

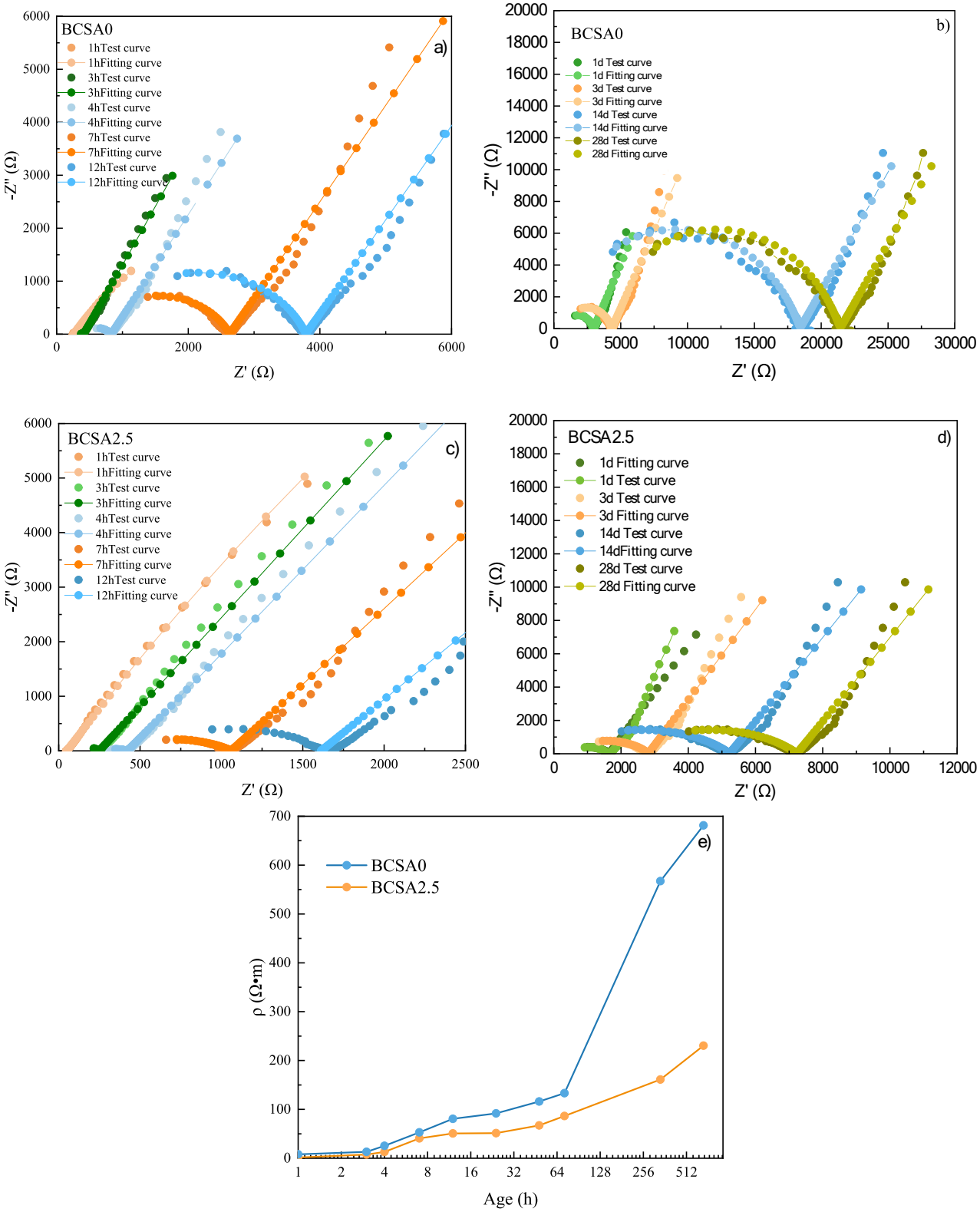

Fig. 3. Nyquist curve of BCAS0 and BCSA2.5 at different curing age.

3.2.2. EIS analysis

Fig. 3a)–d) shows the Nyquist curve of BCAS0 and BCSA2.5 at different curing age, and the resistivity of cement paste can be obtained according to the intersection of the semi-arc and the x-coordinate. The resistivity of BCSA0.25 and BCSA0 from 1 to 28d is shown in Fig. 5f). In principle, the resistivity of cement-based materials can effectively reflect the variation of pore structure and higher pore liquid content [44–46]. It was found that for both pastes that the resistivity increased with time, mainly as the result of the microstructure formation and the subsequent reduction of the connective pores during cement hydration. It was interesting to note that compared with BCSA0, the resistivity of BCSA2.5 significantly reduced throughout the test. On the basis of the isothermal calorimetry test and XRD, it can be assumed that the cumulative of hydration products of BCSA2.5 was more than BCSA0, normally a higher resistivity could be obtained in BCSA2.5. However, considering cobalt itself regarded as a cathode material in lithium batteries, it was reasonable that the electrical conductivity could be significantly enhanced in BCSA pastes with Co(II). This result revealed the potential and possibility of the application of waste cobalt immobilized cement-based materials in specific scenarios that demanding for conductivity, such as the self-sensing concrete or building structural health monitoring.

3.2.3. MIP analysis

Fig. 4 shows the cumulative pore volume and pore size distribution of BCSA pastes at 28 days determined by MIP. It can be seen that the pore volume of pastes slightly decreased when Co(II) was introduced, indicating a general decreasing in porosity of pastes. This can be attributed to the acceleration of BCSA hydration, which led to more hydration products generation thus further densified the microstructure of paste. As for the pore size distribution, the typical bimodal distribution pattern were found for both pastes. It can be seen that for the left-hand peaks (small pore size peak), the pore diameter of the paste containing Co(II) was much smaller than that of the reference group, while for the right-hand peak, the pore diameter for pastes containing Co(II) tended to be larger. As cobalt accelerated the hydration of BCSA, the accumulation of hydration products refined the pore structure, resulting in smaller pore size. The increase in pore size in the medium capillary pores (right-hand peak) may be due to the accumulation of excess of ettringite, which caused possibly micro-cracks.

Previous EIS results showed that the resistivity of BCSA2.5 was significantly reduced compared to BCSA0 throughout the test. Since the differences in pore structure between the two pastes are not significant, this change in resistivity should be attributed to the cobalt-introduced matrix, which was more conductive than the reference sample.

3.2.4. SEM analysis

The SEM images of BCSA pastes with different Co(II) contents at 3d and 28d are present in Fig. 5. Solid matrix is constructed with anhydrous phases (grains), villous spherical particles (AH_3 gels), and needle-shaped hydration products (ettringite) [47]. With the addition of Co(II), a greater amount of hydration products were produced. Consequently, a denser microstructure was formed with a clear increasing amount of ettringite filling the pore spaces of the hardened pastes, as seen in Fig. 5 (b) and (c). This was consistent with the results in sections 3.1 and 3.2 that Co(II) accelerated the hydration of BCSA cement, leading to a higher reaction degree of BCSA cement with more reaction products precipitation. Besides, the evidential result on the denser microstructure of pastes with Co(II) (Fig. 5 (b,c)) than the reference samples (Fig. 5(a)) also confirmed that the results regarding the lower electrical resistivity in BCSA2.5 than that in BCSA0 was due to the high conductivity of Co (II)-bearing phases. Fig. 5(d) is the micrograph of BCSA2.5 at 28d showing the plate-like precipitates. The EDAX results of the plate-like phase are given in Table 3, and the main elements were Ca, Si, Al, with a slight amount of S, Fe, and Co. According to the atomic ratio, the plate-like substance could be attributed to the stratlingite (C_2ASH_8) [18], which was the hydration product formed in the later hydration of BCSA according to Eq. (3). It is noteworthy that the stratlingite was not clearly observed in the XRD pattern of BCSA2.5 at 28d, which can be due to its low in quantity. The presence of Co(II) in the stratlingite indicated that the Co(II) was effectively immobilized in the hydration products.

$$C_2S + AH_3 + 5H \rightarrow C_2ASH_8 \quad (3)$$

3.3. Compressive strength

Fig. 6 shows the compressive strength of BCSA pastes with varied Co (II) concentrations. A slight decrease in compressive strength was found for BCSA pastes with an increase of Co(II) content at 1d. Although the minor differences in compressive strength at 1 day fall within the range of error bars, a slight decrease in early age strength can be observed. This could be due to the rapid accumulation of hydrates, especially ettringite with expansion potential, while the matrix was not yet stiff enough to withstand the expansion, and possibly caused microcracks [48]. In contrast to the reduction of compressive strength found in ordinary Portland cement when applied for Co(II) immobilization, a general positive impact of Co(II) on the compressive strength of BCSA pastes was found in all ages except at 1d. This result was in line with the calorimetry, XRD, and SEM results. It had been verified that Co(II) accelerated the hydration of BCSA, especially ye'elimite according to isothermal calorimetry and XRD results. The faster hydration led to a greater amount of hydration products formation in the matrix compared to the reference group. The needle-shaped ettringite was able to refine the microstructure of the BCSA pastes and reduce the porosity, consequently contributing to the strength development. However, when an excessive amount of Co(II) was introduced, the overload of ettringite might cause an excess of expansion and even microcracks, which finally resulted in a decrease in strength. It can be seen that paste with 0.5% of Co(II)

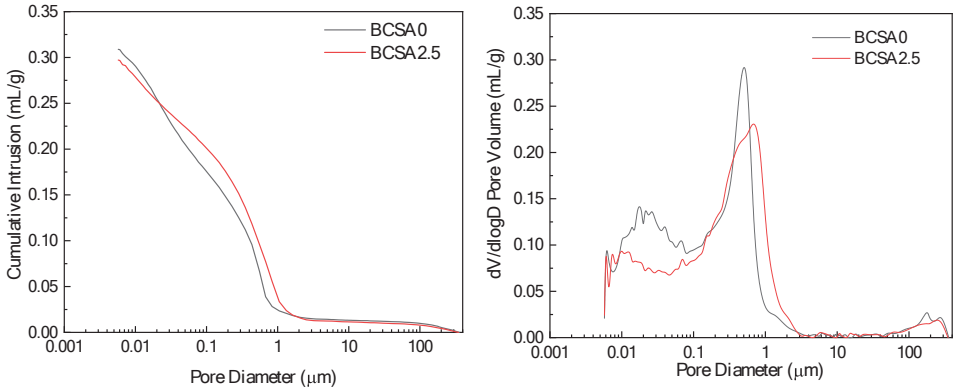

Fig. 4. Cumulative pore volume and pore size distribution of BCSA0 and BCSA 2.5 at 28d.

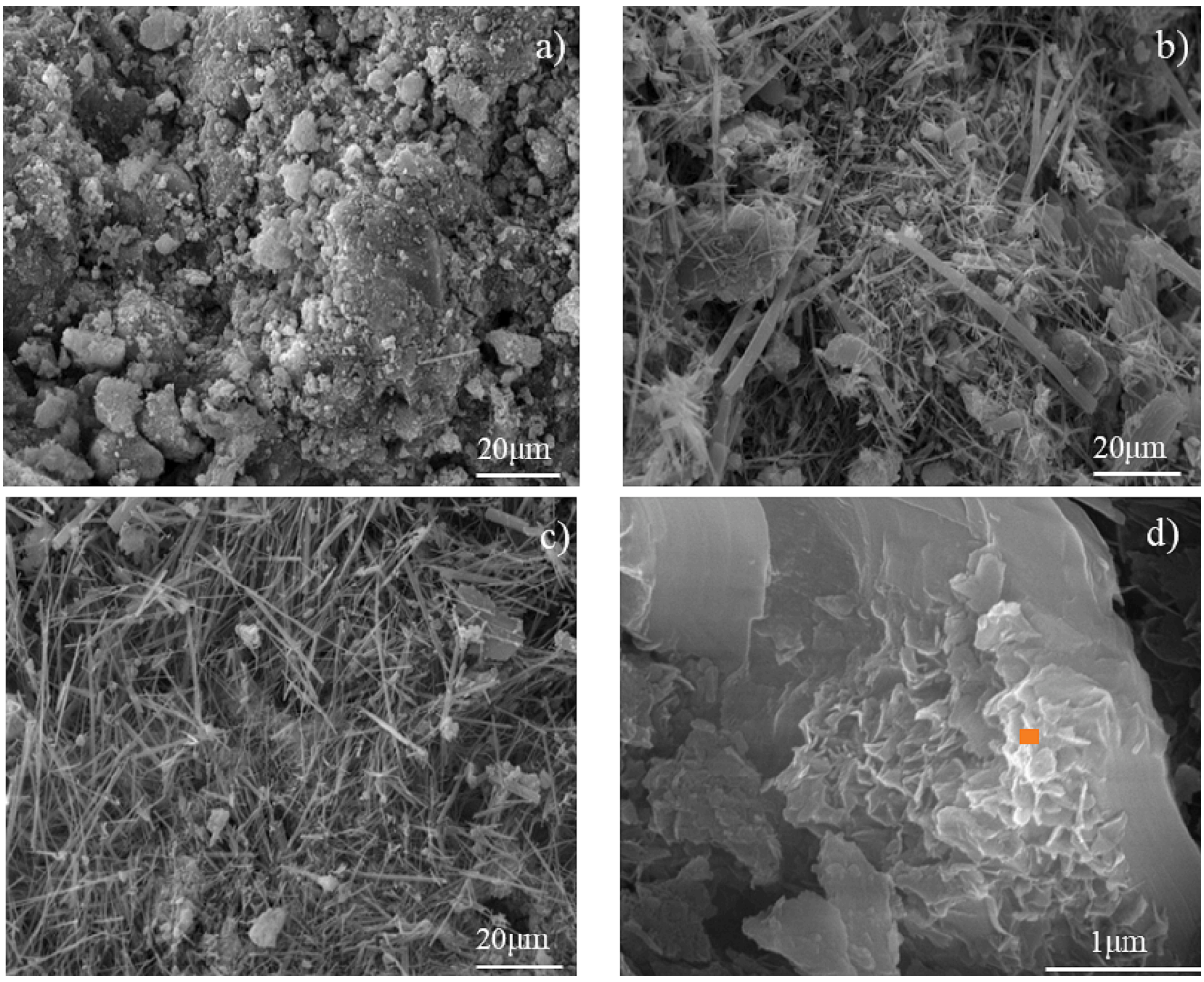

Fig. 5. SEM images of BCSA0 (a), BCSA1(b), BCSA2.5(c) at 3d under 2000x magnifications, and BCSA2.5 at 28d under 80000x magnifications.

Table 3
Atomic ratio of the selected spot.

Element	O K	Al K	Si K	Ca K	S K	Fe K	Co K
At%	24.56	18.56	11.19	38.01	4.85	1.54	1.29

showed the highest compressive strength, whereas BCSA02.5 was found with a minor loss in strength compared with BCSA0.5 but was still equivalent to the reference group.

3.4. Leachability and Immobilization of Co(II)

3.4.1. Immobilization of Co(II)

Fig. 7 records the Co(II) concentration in the $Co(NO_3)_2$ solution blended with BCSA with a liquid to solid ratio of 200:1. The majority of Co(II) was immobilized during the first 100 minutes, as a significant drop of Co(II) concentration was found in the solution. After that, the concentration of Co(II) decreased mildly. As for the concentration of the elements from the BCSA, it can be assumed that the initial dissolution of BCSA cement occurred intensively in ye'elimite, but it occurred mildly in C_2S. This was because the concentrations of Ca, Al, and S were much higher than the concentration of Si during the experimental process. The results were in agreement with the hydration characteristics of the clinker phases of BCSA, in which ye'elimite was the main reactant in the early hydration of BCSA while C_2S promoted the long-term hydration.

The large liquid-to-solid ratio impeded the formation of hardened

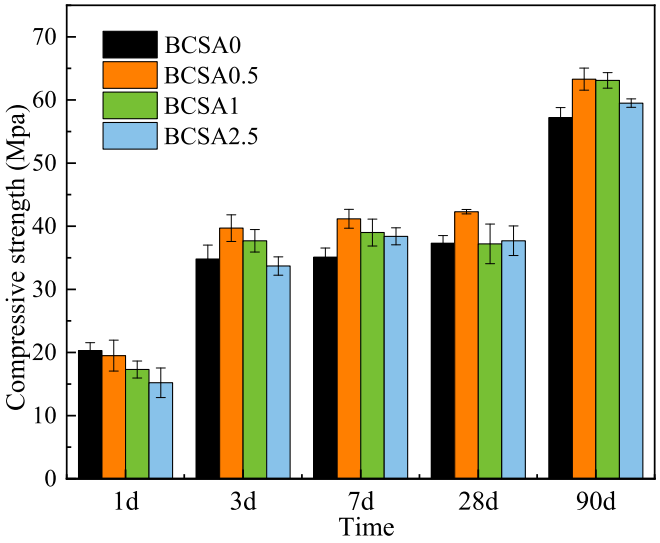

Fig. 6. Compressive strength of BCSA pastes with a varied amount of Co(II).

BCSA pastes, but was beneficial for the dissolution of BCSA. Once the ions concentration reached the oversaturation degree of certain phases, hydrates precipitation would occur. According to the element concentrations in Fig. 6, it can be deduced that the Al-bearing hydrates such as

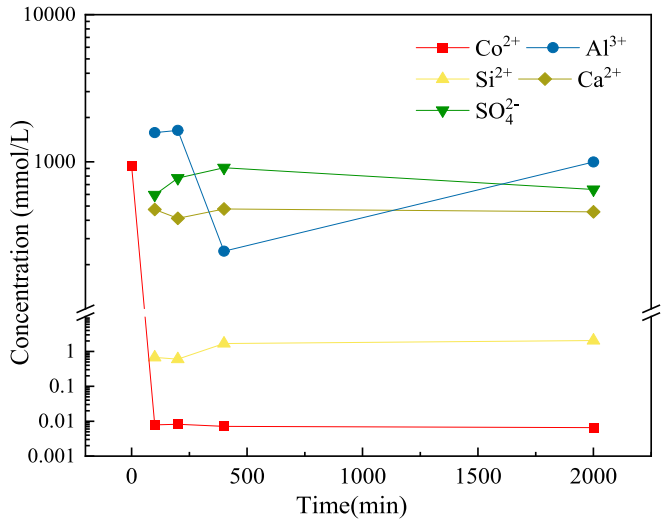

Fig. 7. Ion concentrations of $Co(NO_3)_2$ solution blended with BCSA cement.

ettringite and AH_3 would be generated. The immobilization of Co(II) was, therefore, mainly dependent on the chemical bonding and/or adsorptions by the precipitated hydration products in this experiment. With the satisfactory results obtained on the immobilization of Co(II), it was assured that BCSA showed a superior capacity on the Co(II) immobilization.

3.4.2. Co(II) immobilization degree in BCSA pastes

Fig. 8 depicts the immobilization degrees of Co(II) in BCSA pastes as determined by the TCLP test. The immobilization degrees were calculated by dividing the concentration of immobilized Co(II) from the initial concentration of Co(II) in the mixtures. It could be seen that all mixtures exhibited appealing immobilization degrees of Co(II), and more than 99.75% of Co(II) were immobilized at 1d, irrespective of the Co(II) dosages. Besides, the immobilization degrees increased with curing ages, and achieved the plateau at 7d for all mixtures with a degree at around 99.99%. As the samples were crushed into powders, it was unnecessary to consider the transportation of Co(II) in the hardened BCSA matrix. The hydration products in BCSA were the main functional factor in Co(II) immobilization. Due to the rapid hydration and hydrates precipitation, a substantial amount of hydration products could be generated at 1d, leading to high Co(II) immobilization degrees in the mixtures. The increasing of immobilization degrees of Co(II) with time could be attributed to the increasing of hydration products with time.

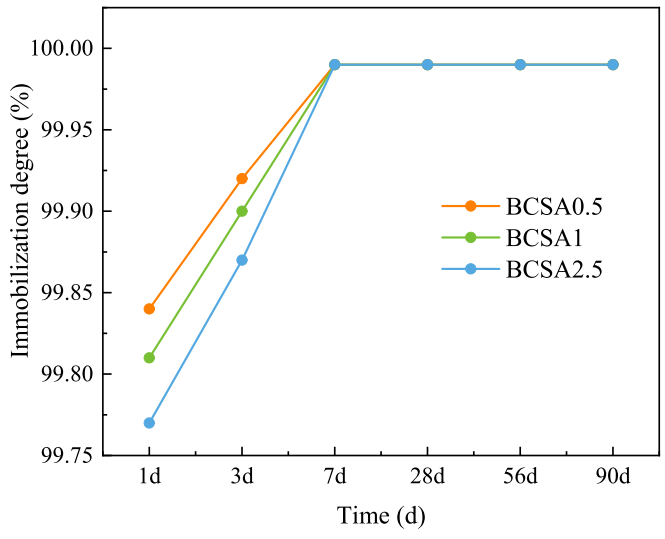

Fig. 8. Immobilization degree of Co(II) in BCSA pastes.

3.4.3. pH on the leaching behavior of Co(II) in BCSA pastes

The environment could strongly influence the leaching behavior of elements during the service life of the cement, and the pH of the environment was one of the main factors. The aqueous concentrations of the elements against pH values are shown in Fig. 9. The concentration of leached Co(II) with pH followed a V-shape pattern. Specifically, the concentration of Co(II) decreased with an increasing pH value of the environment in the pH range of 4-6, subsequently increasing with the increase of pH value in the pH range of 6-11. The reason for the amphoteric leaching pattern of Co(II) could be the amphotericity of cobalt in nature [49]. Similar results were also reported by Mahedi et al. [50] for the leaching of Al, Cu, and Zn. Besides, the increased concentrations of leached Co(II) with the decrease of pH from 6 to 4 could also be because of the dissolving of hydration products in the acid environment. Regardless of the pH value of the environment, the leached Co(II) concentrations were generally low, within the range of 15 mg/L to 20.5 mg/L, and the immobilization degree was greater than 98%.

3.5. Co(II) immobilization mechanism

The experimental results showed that BCSA had a desirable effect on the immobilization of Co(II). The immobilization capacity of BCSA cement depends on the phases compositions of the hydrates as well as the microstructure of the solid matrix. In this paper, the Co(II) immobilization mechanism could be categorized in the following aspects.

(a) Microstructure of BCSA

The leaching test in this research is conducted with crushed BCSA pastes powders. Nonetheless, it is essential to highlight that diffusion is also a major factor determining the Co(II) immobilization capacity in practice. As found in this research that Co(II) accelerated the hydration of BCSA cement, Co(II) contributed to a denser microstructure formation of BCSA pastes with a large amount of hydration products formation, which is beneficial for the immobilization capacity of the matrix as the diffusion pathway of Co(II) would be further blocked. It can be expected that the leaching of Co(II) from the BCSA hardened pastes would be even lower.

(b) Alkaline environment

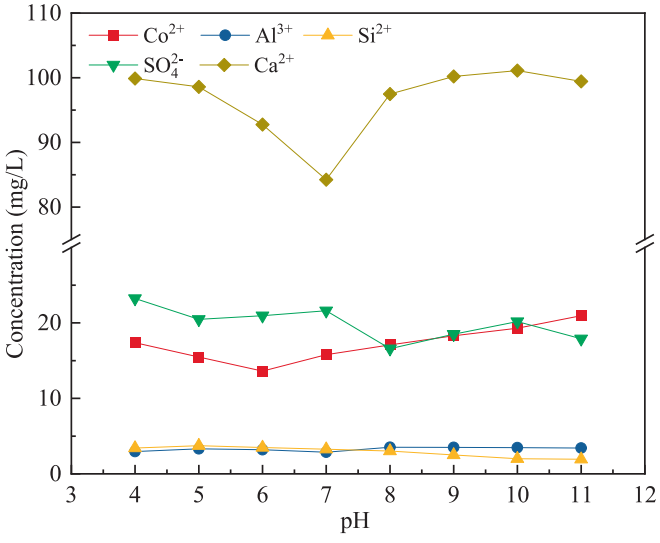

Fig. 9. Effect of pH on the leaching of Co(II), Ca, Si, Al, and S from BCSA 2.5 at 7d.

The alkaline environment is believed advantageous for the immobilization of heavy metals as reported by [51]. A high alkaline environment promoted the precipitation of $Co(OH)_2$, and this chemical immobilization prevents the leaching of Co(II) from the BCSA cement matrix. The pH value of the pore solution of BCSA pastes is with a range of 11.0-12.0, which could possibly lead to the formation of $Co(OH)_2$ and help with the Co(II) immobilization.

(c) Hydration products

Reaction products can play a significant role in Co(II) immobilization. The mechanism of immobilization of heavy metals with hydration products could be summarized as sorption (both physically and chemically) and chemical reaction (ion exchange, surface complexation, diodochy, etc.).

As a primary hydration product, ettringite is the desirable mineral for the hazardous immobilization. Ettringite has the typical needle-shaped structure built up by the octahedral $[Al(OH)_6]^{3-}$ linked with Ca^{2+}, the sulfate and water filled into the channels. It has been reported that the calcium site in the ettringite could be substituted by a variety of divalent cations, and Co(II) in this research could also be implicated [52]. The reaction could be interpreted according to Eq. (4).

$$[Ca_3Al(OH)_6\cdot 12H_2O]_2\cdot(SO_4)_3\cdot 2H_2O + 6Co^{2+} \leftrightarrow [Co_3Al(OH)_6\cdot 12H_2O]_2\cdot(SO_4)_3\cdot 2H_2O + 6Ca^{2+} \quad (4)$$

C-S-H gels are the hydration products that forms in the later stage in BCSA cement and contributes to the long-term strength development. C-S-H gels are highly porous and has a large specific surface area, Co(II) immobilization might be achieved through the sorption of the C-S-H gels. Apart from this, it is reported that the calcium in the 11A tobermorite structures could be partially replaced by Co(II). The ions substitution between Co(II) and calcium in the 11A tobermorite-like C-S-H gels that could be formed in the BCSA cement pastes, therefore, can be effective for Co(II) immobilization [53].

AH_3 gels can immobilize Co(II) through surface complexation. The reaction is simplified as indicated in Eq. (5) [9,54], and the schematic diagram is illustrated in Fig. 10.

$$\equiv AlOH^0 + Co^{2+} \rightleftharpoons \equiv AlOCo^+ + H^+ \quad (5)$$

In addition, the minor hydrates Ca-Al LDH phase identified from the XRD pattern of BCSA pastes are also beneficial for Co(II) immobilization. As illustrated in Fig. 10, the Ca(II) in the Ca-Al LDH would be replaced by Co(II) in the structure to form Co-Al LDH, as the stable crystalline phase in the BCSA pastes.

In summary, Co(II) immobilization in BCSA cement was achieved through multiple mechanisms, including physical/chemical adsorption, precipitation, and ions exchanges [23,25,52,55]. The unbounded Co(II), on the other hand, can also be partially inhibited into the matrix by the densified microstructure, which prevent the leaching of unbonded Co(II) to the external environment [56].

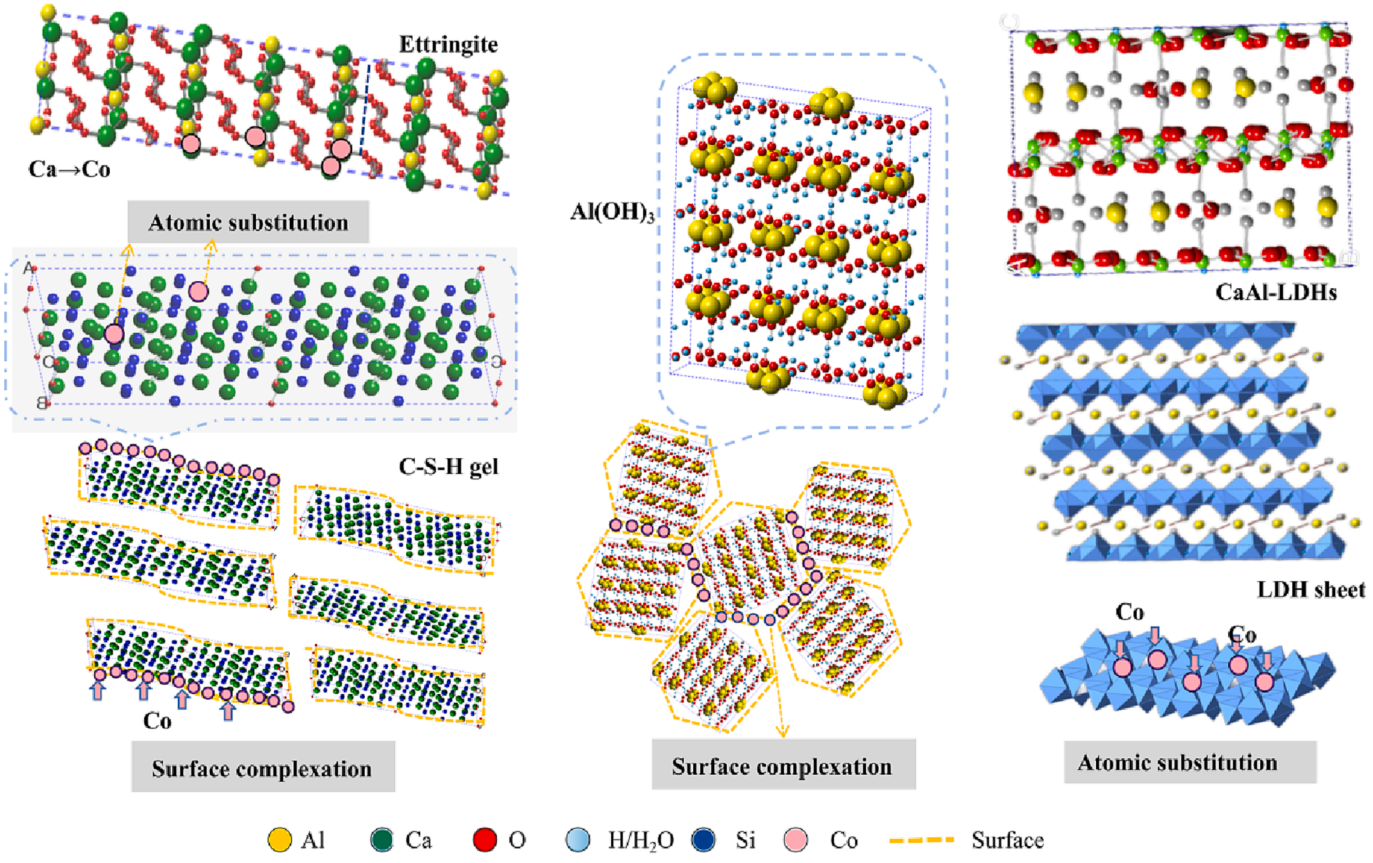

Fig. 10. Schematic diagram of Co(II) immobilization by hydration products and Ca-Al LDH.

4. Conclusions

The objective of this research is to immobilize Co(II) with BCSA, and to understand how Co(II) influences the hydration and strength development of BCSA pastes. The following conclusions could be drawn in this study:

(1) BCSA cement could effectively immobilize Co(II). From the TCLP test, it can be found that the immobilization degrees of Co(II) in BCSA pastes can reach up to 99.9% after 7d of hydration for all of the Co(II) doped BCSA pastes with the Co(II) dosage up to 2.5% by the weight of the BCSA.
(2) Co(II) accelerated the hydration of BCSA cement. With the addition of Co(II), the hydration rate of BCSA cement increased, resulting in the formation of a higher amount of hydration products, which helped to enhance microstructure formation and increase the compressive strength of BCSA cement.
(3) The Co(II)-doped BCSA cement had a lower electrical resistivity than the BCSA cement. This could be a possible advantage for the implication of the BCSA concrete for Co(II) immobilization.
(4) The mechanisms of Co(II) immobilization of BCSA cement are summarized into three aspects based on the microstructure compositions of the BCSA pastes. In this research, the high Co(II) immobilization degrees are mainly attributed to the alkaline environment in the pore solutions and the reactions between Co (II) and hydration products through sorption, ions exchange, and surface complexation.

CRediT authorship contribution statement

Lin Chi: Conceptualization, Writing – original draft, Funding acquisition, Supervision. **Mengxuan Li:** Data curation, Formal analysis. **Qianrui Zhang:** Data curation, Formal analysis. **Xuhui Liang:** Supervision, Writing – original draft. **Chendong Huang:** Visualization, Software, Methodology. **Bin Peng:** Validation, Funding acquisition. **Haisheng Sun:** Data curation.

Declaration of Competing Interest

The authors declare that they have no known competing financial interests or personal relationships that could have appeared to influence the work reported in this paper.

Data availability

Data will be made available on request.

Acknowledgments

This work was supported by the National Natural Science Foundation of China (No. 52208269 & No.51978401) and the Shanghai Sailing Program (No.20YF1431800). Key Laboratory of Performance Evolution and Control for Engineering Structures (Tongji University) (No. 2019KF-5) and the Open Fund of Shanghai Key Laboratory of Engineering Structure Safety (No. 2019-KF07).

References

[1] M. Kosiorek, M. Wyszkowski, Effect of cobalt on the environment and living organisms - a review, Appl. Ecol. Environ. Res. 17 (5) (2019) 11419–11449, https://doi.org/10.15666/aeer/1705_1141911449.
[2] D.G. Barceloux, D. Barceloux, J. Toxicol. – Clin. Toxicol. 37 (2) (1999) 201–216.
[3] G. Lippi, M. Franchini, G.C. Guidi, Blood doping by cobalt. Should we measure cobalt in athletes? J. Occup. Med. Toxicol. 1 (2006) https://doi.org/10.1186/1745-6673-1-18.
[4] M. Oliveira, V.S. Amato, A.B. Lugao, D.F. Parra, Hybrid hydrogels produced by ionizing radiation technique, Radiat. Phys. Chem. 81 (9) (2012) 1471–1474, https://doi.org/10.1016/j.radphyschem.2012.02.004.
[5] L.S. Lawson, J.Q. McComb, R.P. Dong, F.X. Han, C. Roger, Z. Arslan, H.T. Yu, Binding, fractionation, and distribution of Cs Co, and Sr in a US coastal soil under saturated and field capacity moisture regimes, J. Soils Sedim. 16 (2) (2016) 497–508, https://doi.org/10.1007/s11368-015-1228-x.
[6] E.G. Wen, X. Yang, H.B. Chen, S.M. Shaheen, B. Sarkar, S. Xu, H. Song, Y. Liang, J. Rinklebe, D.Y. Hou, Y. Li, F.C. Wu, M. Pohorely, J. Wong, H.L. Wang, Iron-modified biochar and water management regime-induced changes in plant growth, enzyme activities, and phytoavailability of arsenic, cadmium and lead in a paddy soil, J. Hazard. Mater. 407 (2021), https://doi.org/10.1016/j.jhazmat.2020.124344.
[7] H.M. Liu, G.L. Wei, Z. Xu, P. Liu, Y. Li, Quantitative analysis of Fe and Co in Co-substituted magnetite using XPS: The application of non-linear least squares fitting (NLLSF), Appl. Surf. Sci. 389 (2016) 438–446, https://doi.org/10.1016/j.apsusc.2016.07.146.
[8] R. Narendrula, K.K. Nkongolo, P. Beckett, Comparative soil metal analyses in sudbury (Ontario, Canada) and Lubumbashi (Katanga, DR-Congo), Bull. Environ. Contam. Toxicol. 88 (2) (2012) 187–192, https://doi.org/10.1007/s00128-011-0485-7.
[9] L. Chi, Z. Wang, Y. Sun, S. Lu, Y. Yao, Crystalline/amorphous blend identification from cobalt adsorption by layered double hydroxides, Materials 11 (9) (2018), https://doi.org/10.3390/ma11091706.
[10] L. Chi, Z. Wang, Y. Sun, S. Lu, Y. Yao, Removal of cobalt ions from waste water by Friedel's salt, Mater. Res. Express. 6 (1) (2019), https://doi.org/10.1088/2053-1591/aae613.
[11] A.N. Kursunlu, E. Guler, H. Dumrul, O. Kocyigit, I.H. Gubbuk, Chemical modification of silica gel with synthesized new Schiff base derivatives and sorption studies of cobalt (II) and nickel (II), Appl. Surf. Sci. 255 (21) (2009) 8798–8803, https://doi.org/10.1016/j.apsusc.2009.06.055.
[12] E. Assaad, A. Azzouz, D. Nistor, A.V. Ursu, T. Sajin, D.N. Miron, F. Monette, P. Niquette, R. Hausler, Metal removal through synergic coagulation-flocculation using an optimized chitosan-montmorillonite system, Appl. Clay Sci. 37 (3–4) (2007) 258–274, https://doi.org/10.1016/j.clay.2007.02.007.
[13] K.G. Bhattacharyya, S. Sen Gupta, Kaolinite and montmorillonite as adsorbents for Fe(III), Co(II) and Ni(II) in aqueous medium, Appl. Clay Sci. 41 (1–2) (2008) 1–9, https://doi.org/10.1016/j.clay.2007.09.005.
[14] X.J. Liu, J.L. Wu, C. Liu, J.L. Wang, Removal of cobalt ions from aqueous solution by forward osmosis, Sep. Purif. Technol. 177 (2017) 8–20, https://doi.org/10.1016/j.seppur.2016.12.025.
[15] S. Ranganatha, N. Munichandraiah, Synthesis and performance evaluation of novel cobalt hydroxychlorides for electrochemical supercapacitors, J. Solid State Electrochem. 21 (4) (2017) 939–946, https://doi.org/10.1007/s10008-016-3443-9.
[16] I. Smiciklas, S. Dimovic, I. Plecas, M. Mitric, Removal of Co2+ from aqueous solutions by hydroxyapatite, Water Res. 40 (12) (2006) 2267–2274, https://doi.org/10.1016/j.watres.2006.04.031.
[17] H.N. Yoon, J. Seo, S. Kim, H.K. Lee, S. Park, Characterization of blast furnace slag-blended Portland cement for immobilization of Co, Cem. Concr. Res. 134 (2020), https://doi.org/10.1016/j.cemconres.2020.106089.
[18] F. Song, Z. Yu, F. Yang, Y. Liu, Y. Lu, Strätlingite and calcium hemicarboaluminate hydrate in belite-calcium sulphoaluminate cement, CeramicsSilikaty 58 (4) (2014) 269–274.
[19] Q.Y. Chen, M. Tyrer, C.D. Hills, X.M. Yang, P. Carey, Immobilisation of heavy metal in cement-based solidification/stabilisation: a review, Waste Manage. 29 (1) (2009) 390–403, https://doi.org/10.1016/j.wasman.2008.01.019.
[20] E. Hekal, E. Kishar, W. Hegazi, M. Mohamed, Immobilization of Co (II) ions in cement pastes and their effects on the hydration characteristics, J. Mater. Sci. Technol. 27 (1) (2011) 74–80, https://doi.org/10.1016/S1005-0302(11)60029-7.
[21] S. Galluccio, T. Beirau, H. Pöllmann, Maximization of the reuse of industrial residues for the production of eco-friendly CSA-belite clinker, Constr. Build. Mater. 208 (2019) 250–257, https://doi.org/10.1016/j.conbuildmat.2019.02.148.
[22] C.A. Luz, J. Pera, M. Cheriaf, J.C. Rocha, Behaviour of calcium sulfoaluminate cement in presence of high concentrations of chromium salts, Cem. Concr. Res. 37 (4) (2007) 624–629, https://doi.org/10.1016/j.cemconres.2006.11.018.
[23] S. Peysson, J. Pera, M. Chabannet, Immobilization of heavy metals by calcium sulfoaluminate cement, Cem. Concr. Res. 35 (12) (2005) 2261–2270, https://doi.org/10.1016/j.cemconres.2005.03.015.
[24] S. Berger, C. Cau Dit Coumes, P. Le Bescop, D. Damidot, Stabilization of ZnCl2-containing wastes using calcium sulfoaluminate cement: cement hydration, strength development and volume stability, J. Hazard. Mater. 194 (2011) 256–267.
[25] K. Piekkari, K. Ohenoja, V. Isteri, P. Tanskanen, M. Illikainen, Immobilization of heavy metals, selenate, and sulfate from a hazardous industrial side stream by using calcium sulfoaluminate-belite cement, J. Clean. Prod. 258 (2020) 120560, https://doi.org/10.1016/j.jclepro.2020.120560.
[26] C. Belebchouche, K. Moussaceb, A. Tahakourt, A. Ait-Mokhtar, Parameters controlling the release of hazardous waste (Ni2+, Pb2+ and Cr3+) solidified/stabilized by cement-CEM I, Mater. Struct. 48 (7) (2015) 2323–2338, https://doi.org/10.1617/s11527-014-0315-6.
[27] B. Guo, B. Liu, J. Yang, S.G. Zhang, The mechanisms of heavy metal immobilization by cementitious material treatments and thermal treatments: a review, J. Environ. Manage. 193 (2017) 410–422, https://doi.org/10.1016/j.jenvman.2017.02.026.
[28] S. Naamane, Z. Rais, M. Taleb, The effectiveness of the incineration of sewage sludge on the evolution of physicochemical and mechanical properties of Portland cement, Constr. Build. Mater. 112 (2016) 783–789, https://doi.org/10.1016/j.conbuildmat.2016.02.121.
[29] Standard test method for compressive strength of hydraulic cement mortars (using 2-in. or [50-mm] cube specimens), in, 2021, p.

[30] L. Chi, Z. Wang, S. Lu, H. Wang, K.H. Liu, W.D. Liu, Early assessment of hydration and microstructure evolution of belite-calcium sulfoaluminate cement pastes by electrical impedance spectroscopy, Electrochim. Acta 389 (2021), https://doi.org/10.1016/j.electacta.2021.138699.
[31] F. Winnefeld, S. Barlag, Calorimetric and thermogravimetric study on the influence of calcium sulfate on the hydration of ye'elimite, J. Therm. Anal. Calorim. 101 (3) (2010) 949–957, https://doi.org/10.1007/s10973-009-0582-6.
[32] F. Winnefeld, B. Lothenbach, Hydration of calcium sulfoaluminate cements - experimental findings and thermodynamic modelling, Cem. Concr. Res. 40 (8) (2010) 1239–1247, https://doi.org/10.1016/j.cemconres.2009.08.014.
[33] C. Coumes, M. Dhoury, J.B. Champenois, C. Mercier, D. Damidot, Combined effects of lithium and borate ions on the hydration of calcium sulfoaluminate cement, Cem. Concr. Res. 97 (2017) 50–60, https://doi.org/10.1016/j.cemconres.2017.03.006.
[34] M. Gerstig, L. Wadsö, A method based on isothermal calorimetry to quantify the influence of moisture on the hydration rate of young cement pastes, Cem. Concr. Res. 40 (6) (2010) 867–874, https://doi.org/10.1016/j.cemconres.2010.02.005.
[35] F. Yang, F. Pang, J. Xie, W. Wang, W. Wang, Z. Wang, Leaching and solidification behavior of Cu2+, Cr3+ and Cd2+ in the hydration products of calcium sulfoaluminate cement, J. Build. Eng. 46 (2022) 103696, https://doi.org/10.1016/j.jobe.2021.103696.
[36] B. Guo, K. Sasaki, T. Hirajima, Selenite and selenate uptaken in ettringite: immobilization mechanisms, coordination chemistry, and insights from structure, Cem. Concr. Res. 100 (2017) 166–175, https://doi.org/10.1016/j.cemconres.2017.07.004.
[37] M. Niu, G. Li, Y. Wang, Q. Li, L. Han, Z. Song, Comparative study of immobilization and mechanical properties of sulfoaluminate cement and ordinary Portland cement with different heavy metals, Constr. Build. Mater. 193 (2018) 332–343, https://doi.org/10.1016/j.conbuildmat.2018.10.206.
[38] H.N. Yoon, J. Seo, S. Kim, H.K. Lee, S. Park, Characterization of blast furnace slag-blended Portland cement for immobilization of Co, Cem. Concr. Res. 134 (2020) 106089, https://doi.org/10.1016/j.cemconres.2020.106089.
[39] M. Vespa, R. Dähn, D. Grolimund, M. Harfouche, E. Wieland, A.M. Scheidegger, Speciation of heavy metals in cement-stabilized waste forms: a micro-spectroscopic study, J. Geochem. Explor. 88 (1) (2006) 77–80, https://doi.org/10.1016/j.gexplo.2005.08.093.
[40] J. Chang, Y. Zhang, X. Shang, J. Zhao, X. Yu, Effects of amorphous AH3 phase on mechanical properties and hydration process of C4A3S¯-CS¯H2-CH-H2O system, Constr. Build. Mater. 133 (2017) 314–322, https://doi.org/10.1016/j.conbuildmat.2016.11.111.
[41] Y. Zhang, J. Chang, J. Ji, AH3 phase in the hydration product system of AFt-AFm-AH3 in calcium sulfoaluminate cements: a microstructural study, Constr. Build. Mater. 167 (2018) 587–596, https://doi.org/10.1016/j.conbuildmat.2018.02.052.
[42] M. Borštnar, N. Daneu, S. Dolenec, Phase development and hydration kinetics of belite-calcium sulfoaluminate cements at different curing temperatures, Ceram. Int. 46 (18) (2020) 29421–29428.
[43] F. Winnefeld, B. Lothenbach, Hydration of calcium sulfoaluminate cements — experimental findings and thermodynamic modelling, Cem. Concr. Res. 40 (8) (2010) 1239–1247, https://doi.org/10.1016/j.cemconres.2009.08.014.
[44] L. Chi, Z. Wang, S. Lu, D. Zhao, Y. Yao, Development of mathematical models for predicting the compressive strength and hydration process using the EIS impedance of cementitious materials, Constr. Build. Mater. 208 (2019) 659–668, https://doi.org/10.1016/j.conbuildmat.2019.03.056.
[45] L. Chi, W. Li, Z. Li, Z. Wang, S. Lu, Q. Liu, Investigation of the hydration properties of cement with EDTA by alternative current impedance spectroscopy, Cem. Concr. Compos. 126 (2022) 104365, https://doi.org/10.1016/j.cemconcomp.2021.104365.
[46] L. Chi, T. Du, S. Lu, W. Li, M. Wang, Electrochemical impedance spectroscopy monitoring of hydration behaviors of cement with Na2CO3 accelerator, Constr. Build. Mater. 357 (2022) 129374, https://doi.org/10.1016/j.conbuildmat.2022.129374.
[47] F. Song, Z. Yu, F. Yang, Y. Lu, Y. Liu, Microstructure of amorphous aluminum hydroxide in belite-calcium sulfoaluminate cement, Cem. Concr. Res. 71 (2015) 1–6, https://doi.org/10.1016/j.cemconres.2015.01.013.
[48] Z. Yu, Y. Zhao, H. Ba, M. Liu, Synergistic effects of ettringite-based expansive agent and polypropylene fiber on early-age anti-shrinkage and anti-cracking properties of mortars, J. Build. Eng. 39 (2021) 102275, https://doi.org/10.1016/j.jobe.2021.102275.
[49] M. Mahedi, B. Cetin, Leaching of elements from cement activated fly ash and slag amended soils, Chemosphere 235 (2019) 565–574, https://doi.org/10.1016/j.chemosphere.2019.06.178.
[50] M. Mahedi, B. Cetin, A.Y. Dayioglu, Leaching behavior of aluminum, copper, iron and zinc from cement activated fly ash and slag stabilized soils, Waste Manage. 95 (2019) 334–355, https://doi.org/10.1016/j.wasman.2019.06.018.
[51] Q. Yuan, C.J. Shi, G. De Schutter, K. Audenaert, D.H. Deng, Chloride binding of cement-based materials subjected to external chloride environment - a review, Constr. Build. Mater. 23 (1) (2009) 1–13, https://doi.org/10.1016/j.conbuildmat.2008.02.004.
[52] M.L.D. Gougar, B.E. Scheetz, D.M. Roy, Ettringite and C-S–H Portland cement phases for waste ion immobilization: a review, Waste Manage. 16 (4) (1996) 295–303, https://doi.org/10.1016/S0956-053X(96)00072-4.
[53] S. Komarneni, E. Breval, D.M. Roy, R. Roy, Reactions of some calcium silicates with metal cations, Cem. Concr. Res. 18 (2) (1988) 204–220, https://doi.org/10.1016/0008-8846(88)90005-1.
[54] Q. Cui, J. Xu, W. Wang, L. Tan, Y. Cui, T. Wang, G. Li, D. She, J. Zheng, Phosphorus recovery by core-shell γ-Al2O3/Fe3O4 biochar composite from aqueous phosphate solutions, Sci. Total Environ. 729 (2020) 138892, https://doi.org/10.1016/j.scitotenv.2020.138892.
[55] M. Chrysochoou, D. Dermatas, Evaluation of ettringite and hydrocalumite formation for heavy metal immobilization: literature review and experimental study, J. Hazard. Mater. 136 (1) (2006) 20–33, https://doi.org/10.1016/j.jhazmat.2005.11.008.
[56] Z. Giergiczny, A. Krol, Immobilization of heavy metals (Pb, Cu, Cr, Zn, Cd, Mn) in the mineral additions containing concrete composites, J. Hazard. Mater. 160 (2–3) (2008) 247–255, https://doi.org/10.1016/j.jhazmat.2008.03.007.